

1 **Culture of the seaweed *Ulva ohnoi* integrated in a *Solea senegalensis* recirculating system:**
2 **Influence of light and biomass stocking density on macroalgae productivity**

3
4 **Joan Oca^{1*}, Javier Cremades², Patricia Jiménez¹, José Pintado³, Ingrid Masaló¹**

5 ¹Departament d'Enginyeria Agroalimentària i Biotecnologia. Universitat Politècnica de
6 Catalunya - BarcelonaTECH. Esteve Terrades 8, 08860 Castelldefels, Catalunya, Spain.

7 ²Coastal biology research group (BioCost). Centro de Investigaci3n Científicas Avanzadas
8 (CICA). Universidade da Coruña. 15071 A Coruña, Galicia, Spain.

9 ³Instituto de Investigaci3n Mariñas (IIM - CSIC), Eduardo Cabello 6, 36208 Vigo, Galicia, Spain.

10 *Corresponding Author: Joan Oca

11 Telephone: 0034 93 552 12 23

12 Mail: joan.oca@upc.edu

13
14 **ORCID**

15 **Joan Oca:** 0000-0003-0394-881X

16 **Javier Cremades:** 0000-0003-2512-8003

17 **Patricia Jimenez:** 0000-0002-9064-7988

18 **Ingrid Masaló:** 0000-0001-6274-4505

19 **José Pintado:** 0000-0003-3606-341X

20
21 **Acknowledgments**

22 This work was funded by Spanish MINISTERIO DE ECONOMIA Y COMPETITIVIDAD (AGL2013-
23 41868-R).

26 **Culture of the seaweed *Ulva ohnoi* integrated in a *Solea senegalensis* recirculating system:**
27 **Influence of light and biomass stocking density on macroalgae productivity**

28

29 **Joan Oca^{1*}, Javier Cremades², Patricia Jiménez¹, José Pintado³, Ingrid Masaló¹**

30 ¹Departament d'Enginyeria Agroalimentària i Biotecnologia. Universitat Politècnica de
31 Catalunya - BarcelonaTECH. Esteve Terrades 8, 08860 Castelldefels, Catalunya, Spain.

32 ²Coastal biology research group (BioCost). Centro de Investigaci3n Científicas Avanzadas
33 (CICA). Universidade da Coruña. 15071 A Coruña, Galicia, Spain.

34 ³Instituto de Investigaci3n Mariñas (IIM - CSIC), Eduardo Cabello 6, 36208 Vigo, Galicia, Spain.

35 *Corresponding Author: Joan Oca

36 Telephone: 0034 93 552 12 23

37 Mail: joan.oca@upc.edu

38 **Abstract.** A growth model was developed to optimize the management of multi-trophic
39 aquaculture systems by analyzing the influence of light and biomass stocking density (*SD*) in
40 the productivity of *Ulva ohnoi* fed with the effluents from *Solea senegalensis* culture tanks.

41 Experimental growth rates and productivity were determined in three flat bottom algae tanks
42 with different incident photon irradiances (E_0) (163, 280 and 886 $\mu\text{mol m}^{-2} \text{s}^{-1}$), photoperiod
43 12:12h and with stocking densities ranging from 82 to 340 gdw m^{-2} . The distribution of photon
44 irradiance in the algae tanks was estimated as a function of the E_0 and *SD*.

45 The results obtained showed that, the algae exposed to the highest E_0 (886 $\mu\text{mol m}^{-2} \text{s}^{-1}$) and
46 *SD* below 170 gdw m^{-2} experimented a strong decrease in their growth rate, together with
47 morphological changes.

48 The model proposed to estimate the specific growth rate (μ_{NET}), on the basis of E_0 and *SD*,
49 assumed that photosynthetic activity is dependent on the local photon flux density and,
50 therefore, spatially distributed in the tank. The non-linear regression used to estimate the
51 growth kinetic parameters showed a standard deviation of the distance between measured
52 and fitted μ_{NET} data values equal to 0.011 d^{-1} .

53 In terms of biomass productivity per unit area (BP_A) the model shows, for each E_0 level, a
54 trend to increase with *SD*, achieving a maximum BP_A , where *SD* can be considered optimal,
55 and decreasing for higher *SD* values. The optimal *SD* and the maximum BP_A achievable can be
56 also determined as a function of E_0 .

57

58 **Keywords:** *Ulva ohnoi*, IMTA, growth model, productivity, photon irradiance, biomass stocking
59 density

60 **INTRODUCTION**

61 Green seaweeds belonging to genus *Ulva* Linnaeus (Ulvophyceae, Chlorophyta) have been
62 identified as good candidates for filtering fish effluents due to their capacity to be cultured
63 unattached, their wide environmental tolerances (Cohen and Fong 2004; Bolton et al. 2009),
64 together with their high growth rates and high capacity to absorb nitrogen (Jiménez del Río et

65 al. 1996; Mata et al. 2010). Furthermore, *Ulva* is gaining interest as ingredient for animal feeds
66 and as a source of ulvans, sulphated polysaccharides with uses in biomedical tissue
67 engineering, regenerative medicine and drug delivery (Lahaye and Robic 2007; Mata et al.
68 2016). Most of the existing growth models for *Ulva* species have been mainly developed for
69 the management of coasts and estuaries (Bendoricchio et al. 1994; Coffaro and Sfriso 1997;
70 Solidoro et al. 1997; Martins and Marques 2002; Aveytua-Alcázar et al. 2008; Ren et al. 2014).

71 *Ulva ohnoi* M. Hiraoka & S. Shimada has been suggested as one of the most suitable species
72 for land-based cultivation, due to its high growth rates, biomass productivity and nitrogen
73 uptake rates (Yokoyama and Ishihi 2010; Lawton et al. 2013; Angell et al. 2014; Mata et al.
74 2016).

75 *Solea senegalensis* Kaup, 1858, has shown to be an adequate fish species for growing at very
76 high stocking densities, compatible with those needed for its intensive commercial farming
77 (Salas-Leiton et al. 2008). The rising intensive production of this species in Spain, Portugal and
78 France (Morais et al. 2016) has increased the interest on developing specific land-based
79 integrated multitrophic aquaculture (IMTA) technologies to minimize the environmental
80 impact of these activities. The similar range of optimal temperature for *U. ohnoi* and *S.*
81 *senegalensis* cultures, generates great expectations on the feasibility of integrating the
82 production of both species. The main challenges to expand the introduction of this technology
83 are related with the capacity to increase the algae productivity and the nutrient uptake per
84 surface unit, reducing the land area required. Recirculating Aquaculture Systems (RAS) allow
85 the intensification of fish production, as high nutrient concentration in water can be controlled
86 by the flow rate delivered from fish to algae tanks. In these conditions, the light delivered to
87 the algae becomes the main factor determining seaweed productivity.

88 *Effect of light in seaweed growth and productivity*

89 The biomass productivity BP expresses the rate of change in dry biomass B , which is given by
90 the difference between biomass production and biomass loss due to respiration, exudation
91 and mortality, as shown in Eq. 1, where μ_{GROSS} and λ are the specific rates of biomass growth
92 and losses, respectively, expressed in d^{-1} (Duarte and Ferreira 1993; Bendoricchio et al. 1994;
93 Aveytua Alcázar et al. 2008; Duarte et al. 2009).

94

$$BP = \frac{dB}{dt} = (\mu_{GROSS} - \lambda) B \quad (1)$$

95

96 The main limiting factors on μ_{GROSS} are light, temperature (T) and nutrient concentration (N).
97 Their influence can be described with a multiplicative formulation:

98

$$\mu_{GROSS} = \mu_{max} f(E) f(T) f(N) \quad (2)$$

99

100 Where μ_{max} is the maximum specific growth rate, and light is expressed in terms of photon
101 irradiance (E) as μmol of photosynthetic photons per square meter and second ($\mu\text{mol m}^{-2} \text{s}^{-1}$).

102

103 In the case that light is the single limiting variable on growth (e.g. under optimal temperature
104 and not limited nutrient supply), the estimation of the net specific growth rate could be
105 calculated by Eq. 3:

106

$$\mu_{NET} = \mu_{max} f(E) - \lambda \quad (3)$$

107

108

Influence of seaweed stocking density on the light delivered to the culture

109

110

111

112

113

114

115

116

117

Most of the tanks used for seaweed production have opaque walls; this implies that only the light incident to the tank water surface can be delivered to seaweeds. In these conditions, the amount of biomass in the tank is frequently expressed in terms of biomass per unit of water surface or stocking density, which will be referred as SD (in $gdw\ m^{-2}$) for dry biomass or FSD (in $kgfw\ m^{-2}$) for wet biomass. The influence of the SD on the growth of cultured seaweeds is consequential from the light attenuation due to self-shading, that causes light gradients which lead seaweeds to experience different light intensities, depending on their location in the tank. Maximizing the productivity will require a suitable management of seaweed stocking densities, oriented to optimize light distribution along the production process.

118

119

120

The incident photon irradiance to the water surface (E_0) attenuates through the water column, by absorption and scattering, and declines exponentially with depth. The photon irradiance at depth z below the surface $E(z)$ is described by the Lambert-Beer law:

$$E(z) = E_0 \exp(-K' z) \quad (4)$$

121

122

123

124

125

Were K' is the apparent light attenuation constant (m^{-1}) that, in a macroalgae tank, will be determined by the water light extinction coefficient K_0 (m^{-1}), by the seaweed biomass per unit volume B_V , expressed in dry weight per unit volume ($gdw\ m^{-3}$), and by the seaweed light extinction coefficient K_a ($m^2\ gdw^{-1}$), as shown in Eq. 5 (Bendoricchio et al. 1994; Coffaro and Sfriso 1997; Rorrer and Cheney 2004; Ren et al. 2014).

$$K' = K_0 + K_a B_V \quad \rightarrow \quad E(z) = E_0 \exp(-(K_0 + K_a B_V)z) \quad (5)$$

126

127

128

129

K_0 can be determined by the presence of suspended particles as phytoplankton, particulate organic matter and particulate inorganic matter (Ren et al. 2014). Nevertheless, in macroalgae culture tanks, K_0 has a small relative contribution to the K' value due to the high macroalgae biomass.

130

131

132

133

In a well-mixed flat bottom tank, the stocking density SD , expressed as the seaweed dry biomass per surface unit, will be equal to $B_V \times Z$, being Z the maximum water depth. The average photon irradiance (E_{av}) can be calculated in function of E_0 and B_V , by integrating Eq. 5 from $z=0$ to $z=Z$, as shown in Eq. 6.

134

$$\begin{aligned} E_{av} &= \frac{1}{Z} \int_{z=0}^{z=Z} E(z, B_V, E_0) dz = \frac{1}{Z} \int_0^Z E_0 \exp(-(K_0 + K_a B_V) z) dz \\ &= \frac{E_0}{(K_0 Z + K_a SD)} [1 - \exp(-(K_0 Z + K_a SD))] \end{aligned} \quad (6)$$

135

136

Modeling the influence of E_0 and SD in seaweed growth

137

138

139

Some models estimate $f(E)$ as a function of the volume average photon irradiance (E_{av}). However, empirical studies have shown that this kind of models should only be used within an established range of: stocking density, incident photon irradiance and tank geometry. It must

140 be pointed out that algae cultivated in two systems exposed to different E_0 can experience the
141 same E_{av} depending on the SD and the tank geometry, despite differing in the respective
142 fractions of light-limited, light-saturated and light-inhibited cells (Molina Grima et al. 1996;
143 Béchet et al. 2013).

144
145 A second kind of model describes the light dependence of algal photosynthesis by assuming
146 that photosynthetic activity is dependent on the local photon flux density and, therefore,
147 spatially distributed within the tank. The measured activity can be considered to be the
148 volume average of the local activity (Evers 1991; Bendoricchio et al. 1994; Coffaro and Sfriso
149 1997; Yun and Park 2003; Ren et al. 2014). In these models, a Local specific light limitation
150 factor (Lsf) can be calculated in function of depth ($Lsf(z)$) by using a Monod-like function,
151 with a half constant K , coupled with the Lambert-Beer law:

$$Lsf(z) = \frac{E(z)}{K + E(z)} = \frac{E_0}{K \exp((K_0 + K_a B_V) z) + E_0} \quad (7)$$

153 In a flat bottom tank, with maximum water depth Z , the model equation for $f(E)$ can be
154 obtained by integrating Eq. 7 thorough the tank depth:

$$f(E) = \frac{1}{Z} \int_{z=0}^{z=Z} Lsf(z) dz = \frac{1}{(K_0 Z + K_a SD)} \ln \frac{E_0 + K}{K + E_0 \exp(-(K_0 Z + K_a SD))} \quad (8)$$

155
156 The aim of this work is to develop a growth model to analyze the effect of stocking density (SD)
157 and incident photon irradiance (E_0) on the growth of *Ulva ohnoi* in flat bottom tanks fed with
158 the effluents from *Solea senegalensis* tanks in a water recirculating system. The model must
159 provide some guidelines to maximize *Ulva* biomass production by optimizing the management
160 of the stocking densities in the culture tanks.

161

162 MATERIAL AND METHODS

163

164 Seaweed and Fish

165 The thallus of *Ulva ohnoi* were collected at the Ebro Delta, from the bioremediation ponds of
166 an aquaculture facility in “Sant Carles de la Ràpita”, Spain (latitude: 40.62 N, longitude 0.66 E).
167 This species was genetically identified by DNA extraction and PCR amplification of the
168 chloroplast *rbcl* gene following the protocol described in Hayden et al. (2003) with the primers
169 used by Manhart (1994). It was maintained at the Aquaculture Laboratories of the “Universitat
170 Politècnica de Catalunya” in Castelldefels (Spain) for more than 3 years, in indoor tanks fed by
171 water coming from a *S. senegalensis* recirculation aquaculture system (RAS) equipped with
172 biological and mechanical filter, water temperature control, aeration and oxygen supply.

173 The fishes were distributed in two vertical-cylindrical tanks with 1 m diameter and 0.3 m water
174 depth. Each tank contained a total biomass around 12.5 kg, and the average individual size was
175 327 ± 175 g in the first tank and 120 ± 57 g in the second tank. The weekly amount of feed
176 provided to fish was around 600g (120g per day from Monday to Friday). Protein content of
177 feed was 57% and the molar ratio N/P was 12.25.

178

179 *Ulva culture facilities*

180 *Ulva ohnoi* was cultivated in three vertical cylindrical indoor tanks (diameter 64 cm and
181 capacity 90 L) illuminated by LED light sources providing different irradiances to each tank and
182 a 12:12h light:dark photoperiod.

183 The incident photon irradiance E_0 was measured by averaging the irradiance values over the
184 water surface, which decreased from the center to the wall of the tank. The average values
185 were calculated by measuring the photon irradiance along two tank axes, fitting the function
186 $E(r)$, being r the distance from the tank center to a specific point on the water surface, and
187 integrating it from $r=0$ to $r=R$; being R the tank radius, as shown in Eq. 9.

$$E_0 = \frac{1}{\pi R^2} \int_0^R 2\pi r(E(r))dr = \frac{1}{R^2} \int_0^R 2r(E(r))dr \quad (9)$$

188 The obtained E_0 for each tank: 163, 280 and 886 $\mu\text{mol m}^{-2} \text{s}^{-1}$, were called low (L), moderate
189 (M) and high (H) E_0 levels, respectively. The maximal values measured at the center of the
190 tanks, achieved, respectively, 217, 516 and 1162 $\mu\text{mol m}^{-2} \text{s}^{-1}$. Considering the 12 h
191 photoperiod, the total photon irradiances delivered daily to the surface of the tanks were,
192 respectively 7, 12, and 38 mol photons m^{-2} .

193 Water was agitated by continuous aeration through a single air entry (diameter 4mm) placed
194 on the tank bottom center. The air flow rate, measured by a rotameter, was maintained
195 around 6.7 L min^{-1} .

196 Water and nutrients were provided by the effluents of two *S. senegalensis* tanks, drained to a
197 buffer tank with a nitrifying biofilter. Most of the effluent volume was recirculated to the fish
198 tanks, but a small fraction was delivered to the algae tanks by peristaltic pumps along the
199 lighting period. The water returned from the algae tanks to the fish buffer tank through a
200 perforated half pipe vertically fastened to the internal wall of each algae tank, to avoid losing
201 algae fragments. An external overflow system maintained a constant water level in the tank.

202

203 *Control of basic water parameters in tanks*

204 To improve the availability of inorganic carbon in algae tanks, sodium carbonate was weekly
205 provided to maintain alkalinity over 100 $\text{mg L}^{-1} \text{CaCO}_3$, and hydrochloric acid was daily added
206 along the lighting period, to avoid pH levels above 8.5 (Bidwell et al. 1985; Menéndez et al.
207 2001; Lobban and Harrison 2007; Zou 2014).

208 Temperature, Dissolved Oxygen (DO) concentration and pH were measured daily, at the end of
209 the dark period, using portable probes (OxyGuard Handy Polaris and OxyGuard Handy pH). The
210 average values obtained \pm sd were 20.7 \pm 1.3 $^\circ\text{C}$ for temperature, 7.01 \pm 0.7 mg L^{-1} for DO and
211 8.24 \pm 0.35 for pH. Total Ammonia Nitrogen ($\text{NH}_3 + \text{NH}_4^+$) concentrations were measured in fish
212 tanks with a photometer (Palintest), giving values from 0 to 0.24 mg N L^{-1} .

213 Water salinity was measured weakly using a salinity refractometer and fresh water was added
214 to compensate for the water lost by evaporation. The average salinity values were 37.5 \pm 1.0 g
215 L^{-1} .

216 Water samples were taken weekly from the buffer tank and filtered by 0.45 μm membrane
217 filter for N-NO_3^- and P-PO_4^{3-} analysis by spectrophotometric methods. The ultraviolet

218 technique (absorbance at 220 nm and 275 nm) was used for nitrate measure (APHA 1992); and
 219 a colorimetric method based on reduction of phosphomolybdic acid for dissolved inorganic
 220 phosphate (Grasshoff et al. 1999). The average N-NO_3^- and P-PO_4^{3-} concentrations \pm sd in fish
 221 tanks were respectively $21.7 \pm 2.5 \text{ mg L}^{-1}$ and $0.59 \pm 0.088 \text{ mg L}^{-1}$. The concentrations of ammonia
 222 N species and nitrite were considered negligible in relation to nitrate, due to the action of the
 223 biological filter.

224

225 *Nutrient supply to algae tanks*

226 The water flow rate delivered to the low and moderate E_0 tanks was 7 L h^{-1} . For the tank with
 227 the highest E_0 the flow rate was doubled to avoid the N and P flow becoming a limiting factor.
 228 Therefore, the level of N and P load can be estimated about $5.65 \text{ g N m}^{-2} \text{ day}^{-1}$ and 0.153 g P m^{-2}
 229 day^{-1} for low and medium irradiance level tanks, and $11.3 \text{ g N m}^{-2} \text{ day}^{-1}$ and $0.306 \text{ g P m}^{-2} \text{ day}^{-1}$
 230 for the highest irradiance tank.

231

232 *Experimental design*

233 To analyze the influence of light and stocking density on *U. ohnoi* growth, the three tanks with
 234 the different levels of incident photon irradiance E_0 abovementioned (L, M and H) were
 235 combined with three levels of initial fresh-weight stocking densities (FSD_i) conducted in
 236 successive trials, lasting 3 weeks each. Two times per week macroalgae were spun, weighted
 237 and restocked to the initial FSD by removing excess biomass. A sample of the removed excess
 238 biomass was dried at 60°C to determine the ratio fw:dw.

239 The three FSD_i levels were 2.4, 1.6 and 0.8 kgfw m^{-2} . Nevertheless, due to the variability of the
 240 water content in fresh samples, the analysis and the model of *Ulva* growth was not based on
 241 initial and final FSD but in the respective dry-weight stocking densities (SD). In consequence,
 242 in the successive trials, each level of FSD_i will provide a non-negligible range of initial dry
 243 biomass stocking densities (SD_i), as shown in Fig. 1. For this reason, the six measurements
 244 obtained from each FSD_i level will not be considered as replicates but as independent SD_i
 245 values.

246

247

248 *Calculating growth rates and biomass productivity per unit area*

249 The net specific growth rate μ_{NET} (d^{-1}) and the biomass productivity per unit area BP_A (gdw m^{-2}
 250 d^{-1}) were calculated, for each combination $E_0 \times SD_i$, using Eq. 10 and 11 respectively, where
 251 $t_f - t_i$ is the time interval and SD is the stocking density (gdw m^{-2}).

252

$$\mu_{NET} = \frac{[\ln(SD_f) - \ln(SD_i)]}{(t_f - t_i)} \quad (10)$$

253

$$BP_A = \frac{SD_f - SD_i}{(t_f - t_i)} \quad (11)$$

254

255 To relate μ_{NET} and SD , each μ_{NET} value must be associated to a specific stocking density,
256 which can be calculated as the average value of SD_i and SD_f .

257

258 *Estimation of growth model parameters*

259 A model was developed to estimate μ_{NET} on the basis of E_0 and SD in a flat bottom *Ulva* tank.
260 It was assumed that photosynthetic activity is dependent on the local photon flux density Lsf
261 (Eq. 7). The model calculates the photon irradiance limiting factor $f(E)$ by volume averaging
262 the local specific light limitation factor (Eq. 8), and the Net specific growth rate μ_{NET} by
263 assuming light to be the single limiting variable on growth, under a fixed temperature and not
264 limited nutrient supply (Eq. 3).

265 As can be observed in Eq. 3 and 8, the model must include, besides the predictor parameters
266 E_0 and SD , light-transfer-related parameters (K_0 , K_a and Z) and growth kinetic parameters
267 (μ_{max} , K and λ). The water light extinction coefficient (K_0) was estimated by measuring the
268 photon irradiance at different water depths in the tank, with the algae biomass laying on the
269 tank bottom. The biomass light extinction coefficient (K_a) was estimated from the values
270 reported in bibliography (Coffaro and Sfriso 1997; Ren et al. 2014). The growth kinetic
271 parameters μ_{max} , K and λ were estimated using the Gauss-Newton nonlinear regression
272 algorithm to minimize the sum of squares of the residual errors (S), and the normal
273 distribution of the residuals was verified.

274

275 **RESULTS**

276

277 The net specific growth rates (μ_{NET}) measured along the experiment showed, in a general
278 way, a positive correlation with the incident photon irradiance (E_0), and a negative
279 correlation with the stocking densities (SD) (Fig. 2). The measured μ_{NET} values for moderate
280 and low E_0 ranged, respectively, from 0.045 to 0.126 and from 0.007 to 0.081 d^{-1} .
281 Nevertheless, the higher μ_{NET} measured (0.19 d^{-1}) was not obtained with the combination of
282 the highest E_0 and the lower initial stocking densities (SD_i), as could be expected. It was
283 found that, with the highest E_0 , reducing SD_i values below 121 $gdw\ m^{-2}$ does not contribute
284 to increase μ_{NET} (see crosses in Fig. 2). In the trials with those conditions, the color and
285 morphology of the algae experimented strong changes, becoming yellowish and showing
286 fragmentation and signs of sporulation, with reduction of the thallus area. Subsequent essays
287 in the same conditions corroborated this behavior. In these essays, the analysis of *Ulva* tissue
288 showed a decrease on chlorophyll concentration, together with an increase of nitrogen
289 concentration.

290 The biomass productivities per unit area (BP_A) are shown in Fig. 4 (dots). The higher values
291 (40 to 51 $gdw\ m^{-2}\ d^{-1}$) were obtained with the combination of the highest E_0 and SD_i above
292 178 $gdw\ m^{-2}$.

293

294 **DISCUSSION**

295 *Growth rates and biomass productivities*

296 The higher biomass productivities per unit area obtained were very close to those obtained in
 297 culture tanks by Figueroa et al. (2009) and Neori et al. (1991) for *U. lactuca* (46.5 and 55 gdw
 298 m⁻² d⁻¹ respectively); Jiménez del Río et al. (1996) for *U. rigida* (40 gdw m⁻² d⁻¹); and Mata et al.
 299 (2016) for *U. ohnoi* (46.3 gdw m⁻² d⁻¹).

300 Change in colour and morphology with the combination of highest E_0 and the lower SD_i can
 301 be a photoadaptive response to high irradiance, as observed in wild *Ulva* (Falkowski and
 302 LaRoche 1991). Moreover, in algae tanks with continuous water renewal along light period, the
 303 reduction of talus area together with the losses in chlorophyll would contribute to diminish
 304 light attenuation (see Eq. 5), increasing the total photon irradiance delivered to the algae and
 305 contributing to increase the damage. For this reason, the μ_{NET} values corresponding to the
 306 damaged trial (highest E_0 and $SD_i < 121$ gdw m⁻²) were not included in the nonlinear
 307 regression to estimate the kinetic parameters μ_{max} , K and λ . To establish the light threshold
 308 which leads to the damage of the algae, is out of the focus of this work and would require
 309 considering many aspects related with the flow pattern of the algae into the tank, photoperiod
 310 and daily evolution of the incident irradiance.

311 *Predictive model for μ_{NET} on the basis of E_0 and SD*

312 The values of the parameters involved on the model are shown in Table 1. The measured
 313 water light extinction coefficient (1.5 ± 0.5 m⁻¹) was, in average, higher than the values reported
 314 for *Ulva* models in lagoons, likely due to the turbulence produced by aeration in the algae
 315 tanks. Furthermore, the turbidity caused by the management of the fish tanks and the bio-
 316 filter, can influence this value.

317 The non-linear regression used to estimate the growth kinetic parameters, showed a standard
 318 deviation between the measured and the fitted values (S) equal to 0.011 d⁻¹. Eq. 12
 319 incorporates the values of the kinetic parameters and allows estimating μ_{NET} on the basis
 320 of E_0 and SD . The comparison between experimental and predicted results of the model is
 321 shown in Fig. 3.

322 The value obtained for the most sensitive parameter, μ_{max} , was very close to the reported in
 323 literature for *Ulva* growth models (Duke et al. 1989; Bendoricchio et al. 1994; De Guimaraens
 324 et al. 2005; Hadley et al. 2015). It must be highlighted that the kinetic parameter μ_{max} (0.416
 325 d⁻¹) is much higher than the highest measured value of μ_{NET} (0.19 d⁻¹) which was also very
 326 close to the maximum measured values reported by several authors (Coutinho and Zingmark
 327 1993: 0.21 d⁻¹; Neori et al. 1991: 0.18 d⁻¹).

$$\mu_{NET} = \frac{\mu_{max}}{(K_0 Z + K_a SD)} \ln \frac{E_0 + K}{K + E_0 \exp(-(K_0 Z + K_a SD))} - \lambda \quad (12)$$

328

329 *Optimal SD to maximize the biomass productivity per unit area (BP_A)*

330 As can be observed in Fig. 4, with the low and moderate irradiances, the BP_A trends to
 331 increase with SD , achieving a maximum BP_A for an optimal SD and decreasing afterwards.
 332 With the higher E_0 the higher optimal SD and maximum BP_A is achieved. With the highest
 333 photon irradiance it seems to be a minimum SD required to avoid the damage of the seaweed.
 334 In our experiment, with E_0 886 $\mu\text{mol m}^{-2} \text{s}^{-1}$, SD values lower than 170 gdw m⁻² induced
 335 damages in the seaweed.

336 The optimal SD , which provides the maximal biomass productivity for a given E_0 , can be
337 estimated from Eq. 12 and the predicted values of the model are shown in Fig. 5. As an
338 example, the graphic shows that, according to our model, with E_0 $200 \mu\text{mol m}^{-2} \text{s}^{-1}$ the optimal
339 SD would be 186gdw m^{-2} and the BP_A achieved would be about $12.6 \text{gdw m}^{-2} \text{d}^{-1}$ (see arrows
340 in Fig. 5).

341 It must be pointed that *Ulva* biomass per unit volume ($B_V = SD/Z$) is limited by the capacity
342 of the tank aeration system to tumble algal biomass. In our experience, this happens when B_V
343 reaches values above 1000gdw m^{-3} , leading to a worse distribution of the photon irradiance
344 delivered to the algae. Therefore, with high E_0 values, higher water depths (Z) can be needed
345 to achieve the optimal SD without exceeding the mentioned B_V value.

346 The proposed growth model of *U. ohnoi* will be useful to improve the productivity of algae by
347 managing the culture densities in order to maintain SD as close as possible to the optimal
348 value along the production cycle. Furthermore, it can be a reference to evaluate the
349 productivity achieved.

350

351

352 List of symbols

353 BP : Biomass productivity (gdw d^{-1})

354 BP_A : Dry biomass productivity per unit of water surface ($\text{gdw m}^{-2} \text{d}^{-1}$)

355 B_V : Dry biomass per unit volume (gdw m^{-3})

356 E : Photon Irradiance ($\mu\text{mol m}^{-2} \text{s}^{-1}$)

357 E_0 : Incident photon irradiance on surface of water ($\mu\text{mol m}^{-2} \text{s}^{-1}$)

358 E_{av} : Volume average photon irradiance ($\mu\text{mol m}^{-2} \text{s}^{-1}$)

359 FSD : Fresh biomass per unit of water surface (kgfw m^{-2})

360 K : Half constant ($\mu\text{mol m}^{-2} \text{s}^{-1}$)

361 K' : Apparent light attenuation constant (m^{-1})

362 K_0 : Water light extinction coefficient (m^{-1})

363 K_a : Seaweed light extinction coefficient ($\text{m}^2 \text{gdw}^{-1}$)

364 Lsf : Local specific light limitation factor (-)

365 r : Distance to the tank center (m)

366 R : Tank radius (m)

367 SD : Stocking density (gdw m^{-2})

368 z : Distance to water surface (m)

369 Z : Tank water depth (m)

370 z : Water depth (m)

371 λ : Biomass loss specific rate (d^{-1})
372 μ_{GROSS} : Biomass growth specific rate (d^{-1})
373 μ_{max} : Maximum specific growth rate
374 μ_{NET} : Net specific growth rate (d^{-1})

375

376 **Acknowledgments**

377 This work was funded by Spanish MINISTERIO DE ECONOMIA Y COMPETITIVIDAD (AGL2013-
378 41868-R).

379

380 **References**

381 Angell AR, Mata L, de Nys R, Paul NA (2014) Variation in amino acid content and its
382 relationship to nitrogen content and growth rate in *Ulva ohnoi* (Chlorophyta). J Phycol 50: 216–
383 226

384 APHA (1992) Standard Methods for the Examination of Water and Wastewater. 18th Edition,
385 American Public Health Association (APHA), American Water Works Association (AWWA) and
386 Water Pollution Control Federation (WPCF), Washington DC

387 Aveytua-Alcázar L, Camacho-Ibar VF, Souza AJ, Allen JI, Torres R (2008) Modelling
388 *Zosteramarina* and *Ulva* spp. in a coastal lagoon. Ecol Model 218: 354–366

389 Béchet Q, Shilton A, Guieysse B (2013) Modeling the effects of light and temperature on algae
390 growth: State of the art and critical assessment for productivity prediction during outdoor
391 cultivation. Biotechnol Adv 31: 1648–1663

392 Bendoricchio G, Coffaro G, Demarchi C (1994) A trophic model for *Ulva rigida* in the Lagoon of
393 Venice. Ecol Model 75: 485–496

394 Bolton JJ, Robertson-Andersson DV, Shuuluka D, Kandjengo L (2009) Growing *Ulva*
395 (chlorophyta) in integrated systems as a commercial crop for abalone feed in South Africa: A
396 swot analysis. J Appl Phycol 21: 575–583

397 Coffaro G, Sfriso A (1997) Simulation model of *Ulva rigida* growth in shallow water of the
398 Lagoon of Venice. Ecol Model 102: 55–66

399 Cohen, R.A., Fong, P., 2004. Physiological responses of a bloom-forming green macroalga to
400 short-term change in salinity, nutrients, and light help explain its ecological success. Estuaries
401 27: 209–216

402 Coutinho R, Zingmark R (1993) Interactions of light and nitrogen on photosynthesis and growth
403 of the marine macroalga *Ulva curvata* (Kützinger) De Toni. J Exp Mar Biol Ecol 167: 11–19

404 De Guimaraens MA, De MoraesPaiva A, Coutinho R (2005) Modeling *Ulva* spp. dynamics in a
405 tropical upwelling region. Ecol Model 188: 448–460

406 Duarte P, Ferreira JG (1993) A methodology for parameter estimation in seaweed productivity
407 modelling. Hydrobiologia 260: 183-189

- 408 Duarte S, Reig L, Oca J (2009) Measurement of sole activity by digital image analysis. *Aquacult*
409 *Eng* 41: 22–27
- 410 Duke CS, Litaker W, Ramus J (1989) Effect of temperature on nitrogen-limited growth rate and
411 chemical composition of *Ulva curvata* (Ulvales: Chlorophyta). *Mar Biol* 100: 143–150
- 412 Evers EG (1991) A Model for Light-Limited Continuous Cultures: Growth, Shading, and
413 Maintenance. *Biotechnol Bioeng* 38: 245–259
- 414 Falkowski PG, LaRoche J (1991) Acclimation to spectral irradiance in algae. *J Phycol* 27: 8-14
- 415 Figueroa FL, Israel A, Neori A, Martínez B, Malta E, Ang P, Inken S, Marquardt R, Korbee N
416 (2009) Effects of nutrient supply on photosynthesis and pigmentation in *Ulva lactuca*
417 (Chlorophyta): Responses to short-term stress. *Aquat Biol* 7: 173–183
- 418 Grasshoff K, Ehrhardt M, Kremling K (eds) (1999) *Methods of Seawater Analysis*. Third edition,
419 Verlag Chemie, Weinheim
- 420 Hadley S, Wild-Allen K, Johnson C, Macleod C (2015) Modeling macroalgae growth and
421 nutrient dynamics for integrated multi-trophic aquaculture. *J Appl Phycol* 27: 901–916
- 422 Hayden HS, Blomster J, Maggs CA, Silva PC, Stanhope M J, Waaland J R (2003) Linnaeus was
423 right all along: *Ulva* and *Enteromorpha* are not distinct genera. *Eur J Phycol* 38: 277–294
- 424 Jiménez del Río M, Ramazanov Z, García-Reina G (1996) *Ulva rigida* (Ulvales, Chlorophyta) tank
425 culture as biofilters for dissolved inorganic nitrogen from fishpond effluents. *Hydrobiologia*
426 326: 61–66
- 427 Lahaye M, Robic A (2007) Structure and function properties of Ulvan, a polysaccharide from
428 green seaweeds. *Biomacromolecules* 8: 1765–1774
- 429 Lawton RJ, Mata L, de Nys R, Paul NA (2013) Algal bioremediation of waste waters from land-
430 based aquaculture Using *Ulva*: Selecting target species and strains. *PLoS One* 8: e77344.
431 doi:10.1371/journal.pone.0077344
- 432 Lobban CS, Harrison PJ (1994) *Seaweed Ecology and Physiology*. Cambridge University Press,
433 Cambridge
- 434 Manhart J (1994) Phylogenetic analysis of green plant rbcL sequences. *Mol Phylogenet Evol* 3:
435 114–127
- 436 Martins I, Marques JC (2002) A model for the growth of opportunistic macroalgae
437 (*Enteromorpha* sp.) in tidal estuaries. *Estuar Coast Shelf S.* 55: 247–257
- 438 Mata L, Magnusson M, Paul NA, de Nys R (2016) The intensive land-based production of the
439 green seaweeds *Derbesiatenuissima* and *Ulva ohnoi*: biomass and bioproducts. *J Appl Phycol*
440 28: 365–375
- 441 Mata L, Schuenhoff A, Santos R (2010) A direct comparison of the performance of the seaweed
442 biofilters, *Asparagopsis armata* and *Ulva rigida*. *J Appl Phycol* 22: 639–644
- 443 Molina E, Fernández JM, Sánchez JA, García F (1996) A study on simultaneous photolimitation
444 and photoinhibition in dense microalgal cultures taking into account incident and averaged
445 irradiances. *J Biotechnol* 45: 59–69

446 Morais S, Aragão C, Cabrita E, Conceição LEC, Constenla M, Costas B, Dias J, Duncan N, Engrola
447 S, Estevez A, Gisbert E, Mañanós E, Valente LMP, Yúfera M, Dinis MT (2016) New
448 developments and biological insights into the farming of *Solea senegalensis* reinforcing its
449 aquaculture potential. *Rev Aquacult* 8: 227–263

450 Neori A, Cohen I, Gordin H (1991) *Ulva lactuca* biofilter for marine fishpond effluents: II.
451 Growth rate, yield and C:N ratio. *Bot Mar* 34: 389–398

452 Ren JS, Barr NG, Scheuer K, Schiel DR, Zeldis J (2014) A dynamic growth model of macroalgae:
453 Application in an estuary recovering from treated wastewater and earthquake-driven
454 eutrophication. *Estuar Coast Shelf S* 148: 59–69

455 Rorrer GL, Cheney DP (2004) Bioprocess engineering of cell and tissue cultures for marine
456 seaweeds. *Aquacult Eng* 32: 11–41

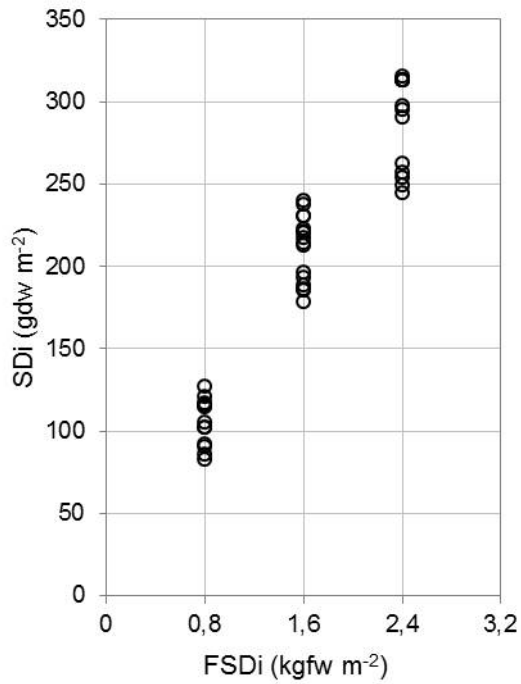
457 Salas-Leiton E, Anguis V, Manchado M, Cañavate JP (2008) Growth, feeding and oxygen
458 consumption of Senegalese sole (*Solea senegalensis*) juveniles stocked at different densities.
459 *Aquaculture* 285: 84–89

460 Solidoro C, Pecenic G, Pastres R, Franco D, Dejak C (1997) Modelling macroalgae (*Ulva rigida*)
461 in the Venice lagoon: Model structure identification and first parameters estimation. *Ecol*
462 *Model* 94: 191–206

463 Yokoyama H, Ishihi Y (2010) Bioindicator and biofilter function of *Ulva* spp. (Chlorophyta) for
464 dissolved inorganic nitrogen discharged from a coastal fish farm - potential role in integrated
465 multi-trophic aquaculture. *Aquaculture* 310: 74–83

466 Yun YS, Park JM (2003) Kinetic modeling of the light-dependent photosynthetic activity of the
467 green microalga *Chlorella vulgaris*. *Biotechnol Bioeng* 83: 303–311

468

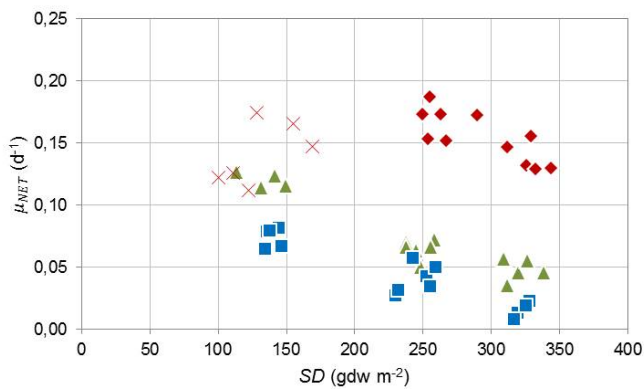


469

470 **Fig. 1** Correspondence between the three levels of initial fresh weight stocking density FSD_i
 471 and the values of initial dry weight stocking density (SD_i) calculated after determining the ratio
 472 dw:fw

473

474

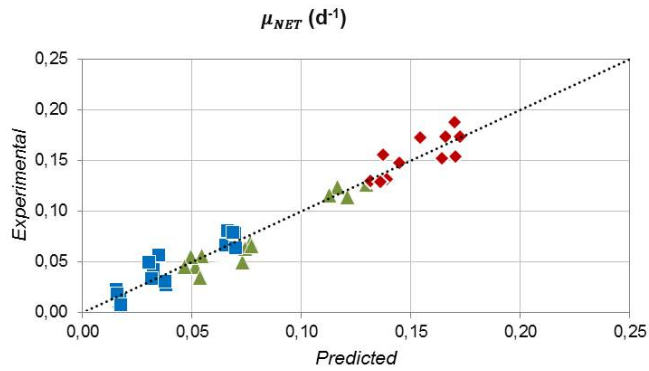


475

476

477 **Fig. 2** Experimental $\mu_{NET}(d^{-1})$ values for the three incident photon irradiances (E_0) 886 (H \blacklozenge),
 478 280 (M \blacktriangle) and 163 $\mu mol m^{-2} s^{-1}$ (L \blacksquare). Red crosses (x) corresponds to the damaged trials with
 479 the highest irradiance

480

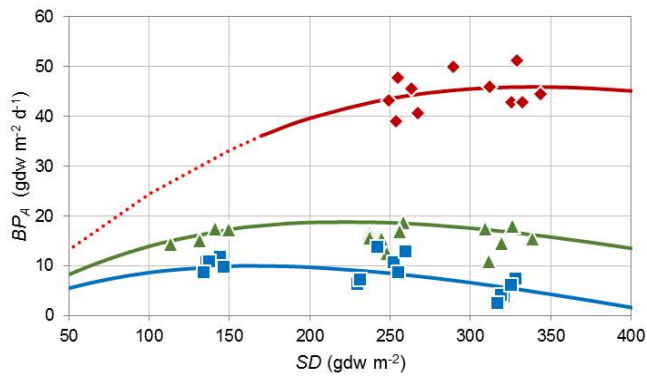


481

482 **Fig. 3** Comparison between experimental and predicted $\mu_{NET}(d^{-1})$ values for the three incident
 483 photon irradiances (E_0) 886 (H \blacklozenge), 280 (M \blacktriangle) and $163 \mu\text{mol m}^{-2} \text{s}^{-1}$ (L \blacksquare)

484

485

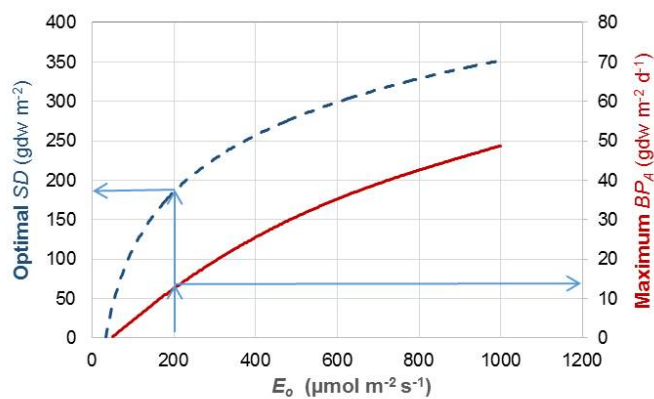


486

487

488 **Fig. 4** Biomass productivity versus SD for the three incident photon irradiances (E_0) 886 (H \blacklozenge),
 489 280 (M \blacktriangle) and $163 \mu\text{mol m}^{-2} \text{s}^{-1}$ (L \blacksquare). Continuous line corresponds to predicted values and
 490 dots to the experimental values. The dotted line indicates the densities which must be avoided
 491 with the highest irradiance to prevent *U/va* damage

492



493

494

495 **Fig. 5** Optimal SD and Maximum BP_A depending on the incident photon irradiance (E_0).
 496 Dashed blue line shows the optimal SD and continuous red line shows the maximum BP_A
 497 achieved. Light blue arrows show, as an example, the optimal SD and Maximum BP_A with E_0
 498 $200 \mu\text{mol m}^{-2} \text{s}^{-1}$

499

500

501

502 **Table 1** Values of the light related and kinematic parameters involved in the estimation of
 503 μ_{NET} from the predictors E_0 and SD . S.E.: Standard error

Symbol	Description of parameter	Value	Units	
<i>LIGHT RELATED PARAMETERS</i>				
K_0	Water light extinction coefficient	1.5	m^{-1}	
K_a	<i>Ulva</i> biomass light extinction coefficient	0.01	$\text{m}^2 \text{gdw}^{-1}$	
Z	Water depth	0.28	m	
<i>ESTIMATED KINEMATIC PARAMETERS</i>				S.E.
μ_{max}	Maximum specific growth rate	0.416	d^{-1}	0.0221
K	Half saturation constant	144.8	$\mu\text{mol m}^{-2} \text{s}^{-1}$	33.64
λ	Specific rate of biomass losses	0.066	d^{-1}	0.0129

504

505

506